Am J Physiol Endocrinol Metab 303: E798–E805, 2012.
First published July 24, 2012; doi:10.1152/ajpendo.00577.2011.

Overexpression of manganese superoxide dismutase ameliorates high-fat diet-induced insulin resistance in rat skeletal muscle

Michael J. Boden,[1]* Amanda E. Brandon,[1]* Jennifer D. Tid-Ang,[1] Elaine Preston,[1] Donna Wilks,[1] Ella Stuart,[1] Mark E. Cleasby,[1,2] Nigel Turner,[1,3] Gregory J. Cooney,[1,3] and Edward W. Kraegen[1,3]

[1]*Diabetes and Obesity Program, Garvan Institute for Medical Research, Darlinghurst, New South Wales, Australia;* [2]*Department of Comparative Biomedical Sciences, Royal Veterinary College, University of London, London, United Kingdom; and* [3]*Faculty of Medicine, University of New South Wales, Sydney, New South Wales, Australia*

Submitted 15 November 2011; accepted in final form 13 July 2012

Boden MJ, Brandon AE, Tid-Ang JD, Preston E, Wilks D, Stuart E, Cleasby ME, Turner N, Cooney GJ, Kraegen EW. Overexpression of manganese superoxide dismutase ameliorates high-fat diet-induced insulin resistance in rat skeletal muscle. *Am J Physiol Endocrinol Metab* 303: E798–E805, 2012. First published July 24, 2012; doi:10.1152/ajpendo.00577.2011.—Elevated mitochondrial reactive oxygen species have been suggested to play a causative role in some forms of muscle insulin resistance. However, the extent of their involvement in the development of diet-induced insulin resistance remains unclear. To investigate, manganese superoxide dismutase (MnSOD), a key mitochondrial-specific enzyme with antioxidant modality, was overexpressed, and the effect on in vivo muscle insulin resistance induced by a high-fat (HF) diet in rats was evaluated. Male Wistar rats were maintained on chow or HF diet. After 3 wk, in vivo electroporation (IVE) of MnSOD expression and empty vectors was undertaken in right and left tibialis cranialis (TC) muscles, respectively. After one more week, insulin action was evaluated using hyperinsulinemic euglycemic clamp, and tissues were subsequently analyzed for antioxidant enzyme capacity and markers of oxidative stress. MnSOD mRNA was overexpressed 4.5-fold, and protein levels were increased by 70%, with protein detected primarily in the mitochondrial fraction of muscle fibers. This was associated with elevated MnSOD and glutathione peroxidase activity, indicating that the overexpressed MnSOD was functionally active. The HF diet significantly reduced whole body and TC muscle insulin action, whereas overexpression of MnSOD in HF diet animals ameliorated this reduction in TC muscle glucose uptake by 50% ($P < 0.05$). Decreased protein carbonylation was seen in MnSOD overexpressing TC muscle in HF-treated animals (20% vs. contralateral control leg, $P < 0.05$), suggesting that this effect was mediated through an altered redox state. Thus interventions causing elevation of mitochondrial antioxidant activity may offer protection against diet-induced insulin resistance in skeletal muscle.

reactive oxygen species; antioxidant; oxidative stress; mitochondria

INSULIN RESISTANCE (NORMALLY ASSOCIATED WITH OBESITY) is an essential prerequisite for development of the metabolic syndrome and type 2 diabetes (47). As little as 3–4 days of high-fat (HF) feeding is sufficient to initiate a state of insulin resistance in rats and humans (1, 2, 35, 49), and there is evidence that insulin resistance occurs in conjunction with an increase in oxidative stress markers, including depleted intracellular glutathione levels, increased mitochondrial hydrogen peroxide production, and an increased intracellular oxidative state (1). Specifically in muscle, impaired insulin-stimulated glucose disposal triggered by a variety of stimuli (hyperinsulinemia, hyperlipidemia, glucocorticoids, and inflammatory cytokines) is associated with increased production of reactive oxygen species (ROS) (29). Intramyocellular ROS are derived primarily from the mitochondria (34, 54), and mitochondria themselves are subject to ROS-induced posttranslational modifications (41). Furthermore, the ROS output of mitochondria increases as ROS-induced posttranslational modifications, such as glutathionylation of complex I, accumulate (50). Once generated, the reactive species (superoxide and hydrogen peroxide, among others) are able to diffuse from the mitochondria and cause damage to other cellular compartments or neighboring tissues.

Nonspecifically targeted antioxidant treatment has offered limited protection or improvement of metabolic function (15). However, the insulin resistance in all of the models described above is ameliorated by the administration of antioxidants that are specifically targeted at or permissive to mitochondrial function (1, 5, 29, 30). The systemic administration of small molecule antioxidants, although beneficial, is too global an intervention to identify the critical tissues involved, and the effects may be limited by poor bioavailability or off-target effects. Similarly, although whole body transgenic models have offered insight into enzymatic control of oxidative stress (11, 27, 58), accurate extrapolation of the specific roles of mitochondrial enzymes is limited by potential developmental effects and lack of tissue specificity inherent in this approach.

The endogenous mitochondrial antioxidant enzyme manganese superoxide dismutase (MnSOD) is upregulated by treatments that improve insulin sensitivity (18, 25, 46) and may be playing a role in the regulation of insulin action. However, interventional studies are needed to explore this possibility. Thus, here we have used in vivo electroporation to achieve transient muscle-specific overexpression of MnSOD to investigate whether HF diet-induced muscle insulin resistance could be ameliorated by local overexpression of MnSOD.

METHODS

Animal housing and maintenance. The study was approved by the Animal Experimentation Ethics Committee of the Garvan Institute for Medical Research/St. Vincent's Hospital and was conducted in accordance with the National Health and Medical Research Council of Australia Guidelines on Animal Experimentation. Male Wistar rats (200 g) were obtained from the Animal Resources Centre (Canning Vale, Western Australia, Australia), maintained at 22 ± 1°C, 55% humidity, on a 12:12-h light-dark photoperiod in the Garvan Institute Specific Pathogen Free Biological Testing Facility, and provided with food and water ad libitum. On arrival, animals were allowed 1 wk to acclimatize before experimentation. Animals were maintained on

* M. J. Boden and A. E. Brandon shared first authorship.
Address for reprint requests and other correspondence: E. W. Kraegen, Diabetes and Obesity Program, Garvan Institute for Medical Research, Darlinghurst, NSW, Australia 2010 (e-mail: e.kraegen@garvan.org.au).

either a normal chow diet (21% protein, 8% fat, 71% carbohydrate, Rat and Mouse Breeder Diet; Gordon Specialty Stockfeeds, Yandarra, New South Wales, Australia) or an in-house-produced HF diet (45% of calories from fat, 20% from protein, and 35% from carbohydrates) based on rodent diet no. D12451 (Research Diets, New Brunswick, NJ) (53).

Vector construction. The muscle-specific mammalian expression vector (EH114) has been described previously (13). A COOH-terminal Myc tag was inserted by PCR onto human MnSOD cDNA (29), and the resultant product was ligated into pGEM-T easy vector (Promega, Madison, WI) before excision using *Eco*RI and subcloning into the EH114 expression vector. All molecular cloning reagents were obtained from Promega or New England Biolabs (Ipswich MA). The MnSOD-Myc construct was transformed into One Shot TOP10 Chemically Competent *E. coli* (Invitrogen, Carlsbad, CA), and stocks of plasmid DNA for electroporation were generated using Endofree plasmid Mega/Giga prep kits (Qiagen, Mississauga, ON, Canada).

IVE and cannulation surgery. IVE was performed 1 wk prior to experimentation, or 3 wk into the 4-wk HF diet administration protocol, as described previously (13). Animals were briefly anesthetized, using 4% isofluorane for induction and 2% for maintenance of anesthesia. The tibialis cranialis (TC) muscles of both legs were pretreated with 45 IU of hyaluronidase (Sigma-Aldrich, St. Louis, MO) administered as 4×25 μl injections distributed along the length of the muscle, and animals were allowed to recover in their cage. Two hours later, under isoflurane anesthesia, 0.5 μg/μl DNA, or empty vector (EH114), was suspended in 0.9% saline and administered into the right and left TC muscles in 6×30 μl injections. Immediately afterward, SignaGel electrode gel (Parker Laboratories, Fairfield, NJ) was applied to the skin, and 1×800 and 4×80 V/cm^2 electrical pulses were generated from an ECM-830 electroporator device (BTX, Holliston, MA) and applied across the distal limbs via a pair of tweezer electrodes. Previous studies from our laboratory have demonstrated that ~50–75% of muscle fibers can be transfected in this way and that, by 7 days post-IVE, protein markers of stress are not elevated (13, 14). Immediately after IVE, both jugular veins were cannulated as described previously (12, 31). Animals were housed individually after surgery, weighed, and handled daily to minimize stress, and those that failed to recover their preoperative weight were not included in the study.

Hyperinsulinemic euglycemic clamp study. Seven days postsurgery, animals were fasted for 5 h, indwelling jugular cannulae were attached to a sampling or infusion line, and hyperinsulinemic euglycemic clamps were performed as described previously (8, 32) using a 0.25 U·kg^{-1}·h^{-1} insulin infusion and a variable glucose infusion rate to maintain euglycemia. During the clamp, blood samples were collected every 10 min, and blood/plasma glucose levels were measured using a YSI 2300 glucose analyzer (YSI, Yellow Springs, OH). Once at steady state, 2-deoxy-D-[2,6-^{3}H]glucose (Amersham Biosciences, Buckinghamshire, UK) was administered as a bolus, followed by collection of blood samples (200 μl) 2, 5, 10, 15, 20, 30, and 45 min later. At completion, animals were euthanized using Nembutal (Abbott Laboratories, Abbott Park, IL), and tissues were rapidly dissected and processed for isolation of mitochondrial/cytosolic fractions or frozen in liquid nitrogen for subsequent analysis. Whole body glucose uptake and glucose uptake into TC muscles (Rg′) were calculated as described previously (36).

Plasma hormone and metabolite analysis. Plasma insulin was assayed using a rat insulin RIA kit (Millipore, Billerica, MA). Plasma triglycerides were evaluated using a triglyceride GPO-PAP kit (Roche Diagnostics, Indianapolis, IN) and nonesterified fatty acids using a NEFA-C kit (WAKO Pure Chemical Industries, Chuo-ku, Osaka, Japan).

Tissue gene expression analysis. Extraction of mRNA from electroporated muscle was performed using TRI-Reagent (Sigma-Aldrich) per the manufacturer's instructions. RNA was converted to cDNA using Omniscript RT-Kit (Qiagen) and expression of total (rat and human) MnSOD (forward 5′-AACGCGCAGATCCAG-3′, reverse 5′-CCTTTGGGTTCTCCACCAC-3′, UPL probe no. 41) and cyclophilin (forward 5′-TGCTGGACCAAACACAAATG-3′, reverse 5′-CTTCCCAAAGACCACATGCT-3′, UPL probe no. 42) evaluated using the Universal Probe Library RT-PCR assay and 480 LightCycler (Roche Diagnostics). The expression of total MnSOD was normalized to the expression of cyclophilin using the $-\Delta\Delta C_T$ method, as described previously (33, 37).

Muscle fractionation. The processing of tissues for mitochondrial/cytosolic fractionation is detailed in Ref. 9. Briefly, excised tissues were homogenized in ice-cold isolation buffer (100 mM sucrose, 100 mM KCl, 50 mM Tris·HCl, 1 mM KH_2PO_4, and 0.1 mM EGTA, pH 7.0) using a Polytron (Kinematica, Littau, Switzerland). Samples were diluted in isolation buffer and centrifuged to pellet debris before separation into mitochondrial and cytosolic fractions by differential centrifugation. Integrity of fractions was verified by Western blotting for voltage-dependent anion channel and lactate dehydrogenase, markers for mitochondrial and cytosolic fractions, respectively.

SDS-PAGE and Western blotting. Samples were homogenized in RIPA buffer (65 mM Tris·HCl, 150 mM NaCl, 5 mM EDTA, 1% NP-40, 0.5% Na-deoxycholate, 0.1% SDS, and 10% glycerol, pH 7.4) containing protease and phosphatase inhibitors (1 μg/ml aprotinin, 1 μg/ml leupeptin, 10 mM NaF, 1 mM Na_3VO_4, and 1 mM PMSF). Samples were incubated at 4°C for 2 h with agitation before centrifugation for 10 min at 16,000 *g*. Supernatant was collected and assayed for protein content using the Bradford protein assay (Bio-Rad, Hercules, CA). Samples were subjected to SDS-PAGE, transferred to polyvinylidene difluoride (PVDF) membranes (GE Healthcare, Buckinghamshire, UK), and blocked with 1% BSA (Invitrogen, Carlsbad, CA) before application of primary and secondary antibodies and visualization with Western Lightning ECL reagent (Bio-Rad). Antibodies for MnSOD were from Santa Cruz Biotechnology (Santa Cruz, CA). Mitochondrial respiratory chain subunits (complex I subunit NDUFB6, complex II FeS subunit, complex III Core2 subunit, and complex V subunit-α; MS601) were from Mitosciences (Eugene, OR). All other primary antibodies were sourced from Cell Signaling Technology (Danvers, MA), and all secondary antibodies were from Jackson ImmunoResearch (West Grove, PA).

Enzyme activity and protein carbonylation assays. Muscle was prepared for enzyme assay by homogenization at a 1:20 dilution in enzyme assay buffer (50 mM Tris·HCl buffer, 0.1% Triton X-100, and 1 mM EDTA, pH 7.4) using a mortar and pestle and subjected to three freeze-thaw cycles before being centrifuged at 16,000 *g* for 10 min at 4°C. The supernatant was transferred to a fresh tube and stored at −80°C. All reagents were obtained from Sigma-Aldrich unless otherwise stated.

MnSOD activity was measured spectrophotometrically using a modification of the protocol of Floche and Otting (21). Reaction buffer (50 mM sodium phosphate, 0.1 mM EDTA, 0.01 mM cytochrome *c*, and 0.01 mM xanthine, pH 7.8, 25°C) was mixed with xanthine oxidase (0.005 units) and sodium cyanide (final cuvette concentration, 2 mM), and the change in absorbance at 550 nm was followed. Sample was then added stepwise (in 20-μl increments at a concentration of 5–10 mg/ml), and the concentration of sample required to decrease the rate of reaction by 50% (defined as 1 unit of MnSOD activity) was calculated. MnSOD activity was expressed as units of MnSOD activity per milligram of protein. Citrate synthase activity was measured per the method of MacArthur et al. (39). Glutathione peroxidise activity was measured spectrophotometrically using the protocol of Flohe and Gunzler (20). Catalase activity was measured using the protocol modified from Beers and Sizer (4); 1.9 ml of 50 mM potassium phosphate buffer (pH 7) and 75 μl of sample were equilibrated to 30°C in a quartz cuvette. A baseline reading was taken before addition of 25 μl of 1 M H_2O_2 in phosphate buffer, and reaction rate followed at 240 nm. The extinction coefficient of H_2O_2 was 0.0436 μmol·ml^{-1}·cm^{-1}.

Assay of protein carbonylation in muscle lysates was performed using an OxyBlot Protein Oxidation Detection Kit (Millipore) per the

manufacturer's instructions. Using the primary antibody from the OxyBlot kit, we immunoprecipitated all carbonylated proteins from 2,4-dinitrophenylhydrazine-derived lysates (250 μg). Immunoblotting was then carried out for insulin receptor substrate-1 (IRS-1) and Akt. Akt was also immunoprecipitated from nonderived lysates (500 μg), subjected to SDS-PAGE, and transferred to PVDF membranes, as described above. Before blocking, membranes were derived using the method of Dalle-Donne et al. (16). Carbonylation was then determined using the primary antibody from the OxyBlot kit.

Statistics. Statistical analyses were performed using GraphPad Prism (GraphPad Software, San Diego, CA). Differences between electroporated and nonelectroporated muscles were assessed by paired Student *t*-tests. Otherwise, an unpaired Student's *t*-test or ANOVA (mixed model) was used together with Fisher's protected least significant difference post hoc tests as appropriate. $P < 0.05$ was considered significant. Data are reported as means ± SE unless otherwise stated.

RESULTS

MnSOD overexpression in skeletal muscle. IVE using the MnSOD-Myc construct increased total MnSOD mRNA 4.5-fold at 7 days postelectroporation compared with the contralat-

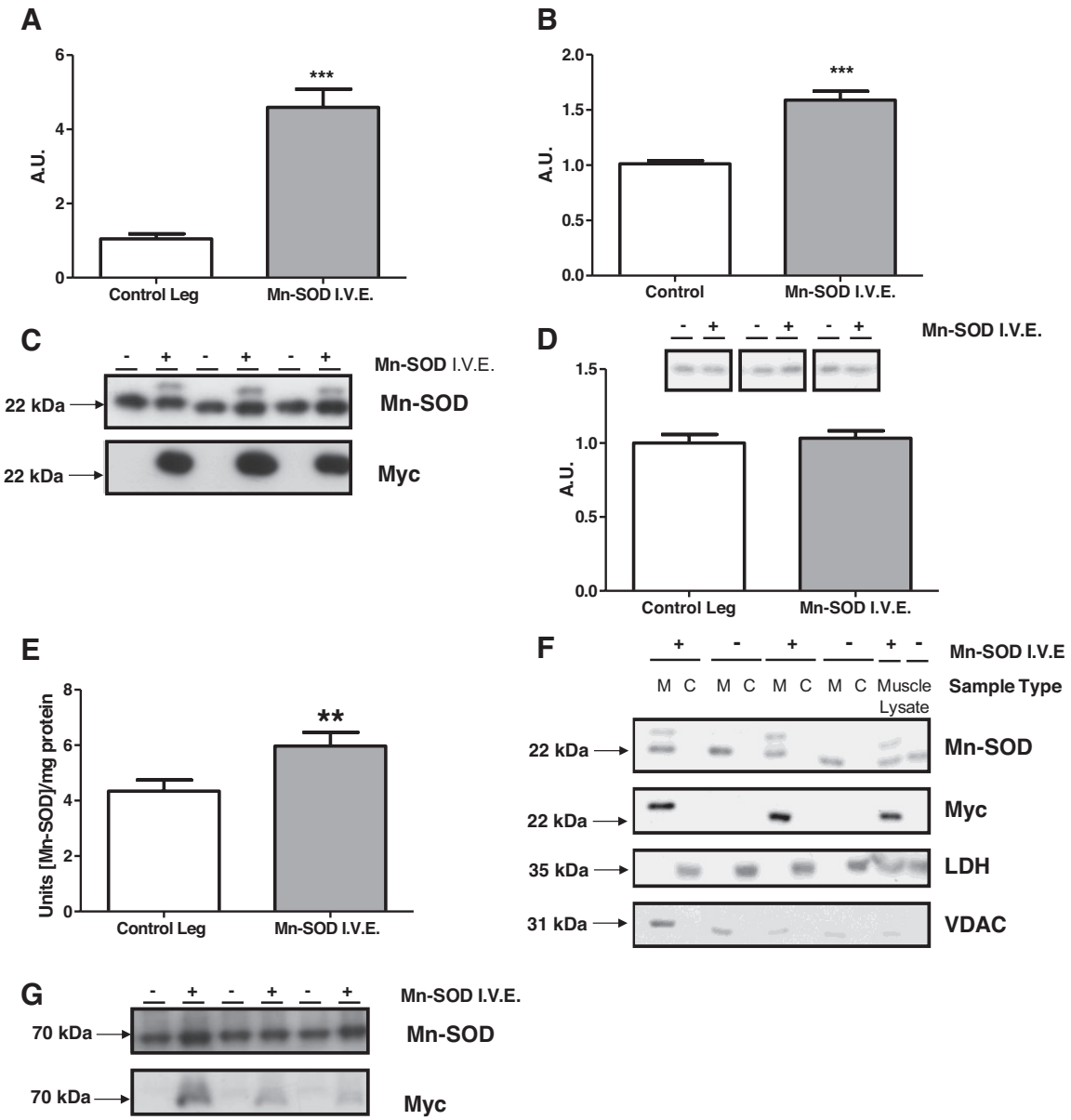

Fig. 1. Successful overexpression of manganese superoxide dismutase (MnSOD) in TC muscle. *A*: mRNA expression of endogenous and exogenous *mnsod* in control and MnSOD in vivo electroporation (IVE) tibialis cranialis (TC) muscle ($n = 9$/group). *B*: protein expression in whole muscle lysates of endogenous and exogenous MnSOD; $n = 9$/group. *C*: Western blots of whole muscle lysates comparing expression of endogenous and exogenous MnSOD protein. *D*: protein expression in whole muscle lysates of Cu/Zn-SOD ($n = 6$/group). *E*: whole muscle lysate activity assay for MnSOD. Enzyme activity measured by spectrophotometer ($n = 6–8$/group). *F*: Western blots of mitochondria-enriched, cytosol-enriched, and total muscle lysates from control and MnSOD IVE TC muscle. Blots with antibodies to MnSOD (22 and 24 kDa for endogenous and exogenous MnSOD, respectively), Myc tag (construct MnSOD only), lactate dehydrogenase (cytosolic marker), and voltage-dependent anion channel (VDAC)/porin (mitochondrial marker) are shown. *G*: Western blots using less stringent denaturing of control and MnSOD IVE TC muscle. High-molecular-weight tetramer is visualized using antibodies for MnSOD (all samples) and using the anti-Myc antibody (MnSOD IVE samples only). ***$P < 0.001$; **$P < 0.01$.

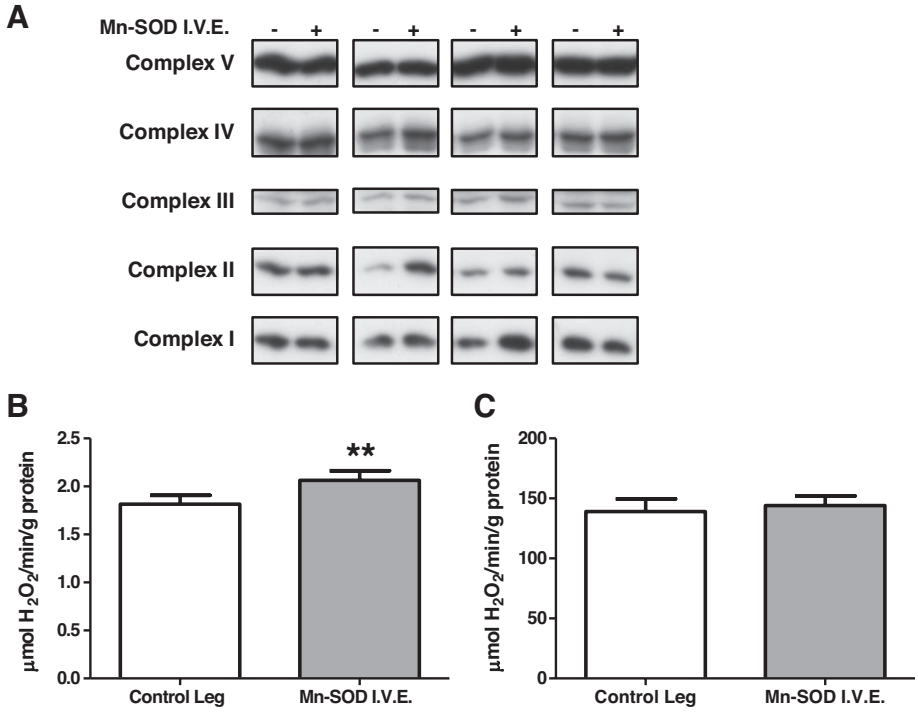

Fig. 2. Downstream changes due to MnSOD overexpression. *A*: representative protein expression by Western blot showing expression of subunits of the electron transport chain complex I, complex II, complex III, complex IV, and complex V. Whole muscle lysate activity assay for glutathione peroxidase (*B*) and catalase (*C*). Enzyme activity was measured by spectrophotometer ($n = 6–8$/group). $^{**}P < 0.01$.

eral muscle ($P < 0.001$; Fig. 1*A*), whereas total MnSOD protein expression was increased by 70% ($P < 0.001$; Fig. 1*B*). The addition of the Myc tag to the MnSOD construct resulted in a minor band shift in the translated protein, but the expression of the human (h)MnSOD construct did not influence the protein expression of endogenous MnSOD (Fig. 1*C*) or the cytosolic superoxide dismutase Cu/Zn-SOD (Fig. 1*D*). The increase in MnSOD protein expression was associated with an increase in MnSOD-specific activity ($P < 0.01$; Fig. 1*E*), confirming that the MnSOD-Myc protein had been functionally overexpressed. Fractionation of muscles into mitochondria-enriched and cytosol-enriched lysates demonstrated that the exogenous hMnSOD protein was expressed primarily within the mitochondrial fraction (Fig. 1*F*), implying that addition of the COOH-terminal Myc tag had not impaired cellular localization of hMnSOD. When exposed to less stringent denaturing conditions, MnSOD retained its 80-kDa tetrameric quaternary structure (Fig. 1*G*). In MnSOD-electroporated tissues, this tetramer was present and contained Myc-tagged protein(s), confirming that exogenous hMnSOD was able to form tetramers of the appropriate size with other MnSOD proteins.

MnSOD overexpression in muscle altered cellular redox state. There were no differences in protein levels of mitochondrial electron transport chain components in MnSOD overexpressing muscle compared with controls (Fig. 2*A*), suggesting that overexpression of MnSOD did not significantly influence mitochondrial mass. However, consistent with enhanced production of hydrogen peroxide as a result of MnSOD overexpression, we observed an increase in activity of the high-affinity hydrogen peroxide-degrading enzyme glutathione peroxidase (Fig. 2*B*) but not of the lower-affinity catalase (Fig. 2*C*). This suggests that a small increase in the activity of enzymes regulating hydrogen peroxide levels was sufficient to maintain intracellular homeostasis.

Diet-induced impairment in insulin-stimulated muscle glucose uptake was ameliorated by MnSOD overexpression. Consumption of a HF diet for 4 wk was sufficient to drive changes in whole body metabolism, resulting in significant increases in adipose depot size and a small but significant increase in overall body weight (Table 1). The HF diet-fed animals required a reduced rate of glucose infusion to maintain euglycemia during a hyperinsulinemic euglycemic clamp and displayed a reduced rate of glucose tracer clearance from plasma, indicative of whole body and peripheral insulin resistance, respectively (Table 1). In addition, the failure of the infused insulin to fully suppress hepatic glucose output implied a concurrent impairment in hepatic insulin action. As expected, the HF diet significantly reduced glucose uptake into TC muscles (by 30%; Fig. 3). Although overexpression of MnSOD did not alter glucose uptake into chow-fed muscle, it was able to increase glucose uptake in HF diet-fed muscle, effectively halving the impairment in glucose uptake observed in control

Table 1. *Euglycemic clamp data of rats fed chow or high-fat diet for 4 wk*

	Chow	High Fat	*P* Value (Vs. Chow Group)
Body weight, g	355 ± 7.6	375 ± 7.6	<0.05
Plasma glucose, mmol/l	8 ± 0.2	7.9 ± 0.3	
Plasma insulin, mU/l	128 ± 12	132 ± 10.7	
Glucose infusion rate, $mg \cdot kg^{-1} \cdot min^{-1}$	34.7 ± 1.8	22.4 ± 2.2	<0.01
Glucose disposal rate, $mg \cdot kg^{-1} \cdot min^{-1}$	37.5 ± 3.0	24.7 ± 2.8	<0.01
Hepatic glucose output, $mg \cdot kg^{-1} \cdot min^{-1}$	−0.52 ± 2.1	5.1 ± 2.8	<0.05
Epididymal fat, g	2.2 ± 0.17	3.1 ± 0.13	<0.01
Retroperitoneal fat, g	1.5 ± 0.14	2.5 ± 0.17	<0.01

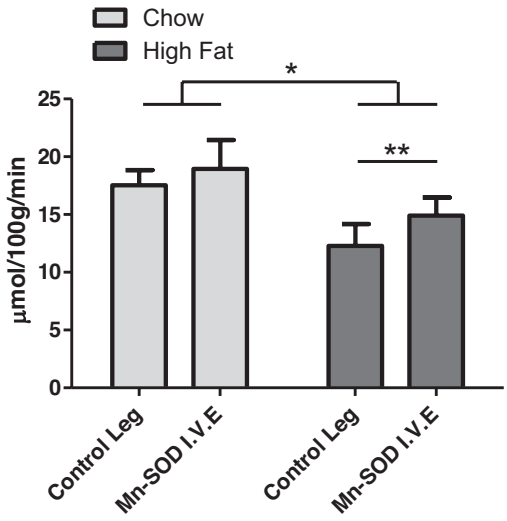

Fig. 3. MnSOD overexpression ameliorates the reduction in glucose uptake due to high-fat diet. Glucose uptake into muscle (Rg′) of chow- and high-fat-fed rats as determined by 2-[^{3}H]deoxyglucose radiolabeled tracer uptake into control and MnSOD IVE TC muscle under euglycemic hyperinsulinemic clamp conditions (n = 6/group) *$P < 0.05$; **$P < 0.01$.

muscles from HF diet-fed rats (Fig. 3). These changes in glucose flux were not accompanied by any significant changes in phosphorylation of phosphatidylinositol (PI) 3-kinase signaling intermediates (p-Y612/IRS-1, p-S473/Akt, p-T642/AS160, and p-S9/GSK-3β) in muscle collected at the end of the clamp (data not shown).

MnSOD overexpression decreased levels of skeletal muscle protein carbonylation in HF diet-treated animals. In chow-fed animals, overexpression of MnSOD did not significantly decrease the level of protein carbonylation. However, HF diet-fed animals demonstrated an increase in levels of protein carbonylation, which were reduced as a result of MnSOD overexpression (Fig. 4). This suggests that MnSOD overexpression was able to reduce the accumulation of ROS-induced posttranslational modifications of protein targets within the muscle. Using immunoprecipitation of carbonylated proteins and blotting for IRS-1 and Akt, we did not show any carbonylation of these proteins involved in insulin signaling (data not shown).

DISCUSSION

The main findings of the present study were that overexpression of MnSOD in a rat skeletal muscle in vivo was able to alleviate HF diet-induced insulin resistance in this same muscle. This change was associated with a reduction in intracellular protein carbonylation. This supports a role for increased ROS production in the generation or maintenance of diet-induced muscle insulin resistance in the rat.

The reactive oxygen species superoxide, produced in muscle primarily by electron leakage from complex 1 and complex 3 of the mitochondrial electron transport chain (34, 54), will react with and deactivate Fe-S cluster proteins (3, 42, 43), result in the generation of other reactive oxygen species such as hydrogen peroxide and peroxynitrite, and thus cause damage to mitochondrial and other proteins. In this study, we have shown that overexpressed exogenous MnSOD protein can be successfully localized to the mitochondria, the primary source of skeletal muscle superoxide generation. The consequent increase in mitochondrial MnSOD activity within the target muscle would be expected to decrease the quantity of superoxide that is able to diffuse out of the mitochondria, thus limiting ROS-induced damage to cellular components.

The beneficial effect of increased MnSOD activity may be tempered by an increased intracellular concentration of hydrogen peroxide if this is not ameliorated by increased glutathione peroxidase or catalase activity. However, it has been reported that elevated hydrogen peroxide production may drive an increase in the activity of glutathione peroxidase and catalase (22). In this study, a small increase in glutathione peroxidase activity was observed without an observable change in catalase activity. In addition, MnSOD overexpression did not result in increased mitochondrial biogenesis, indicated by unchanged levels of electron transport chain components. These observations are consistent with only a minor elevation in cytosolic hydrogen peroxide levels. A minor increase in cytosolic hydrogen peroxide has previously been reported to increase insulin sensitivity in vivo, whereas lowering levels of hydrogen peroxide has the opposite effect (38, 40). Thus, it may be that the improvement in insulin-stimulated muscle glucose uptake observed in the HF diet-fed animals in this study may be underpinned by a mild increase in cellular hydrogen peroxide rather than the observed decrease in levels of superoxide and protein carbonylation.

Exposure to a HF diet caused a decrease in glucose uptake into muscle, which MnSOD overexpression was able to ameliorate significantly. This indicates that even the comparatively moderate increase in MnSOD expression achieved in this study [compared with the 2.5-fold increase in expression generated previously in myotubes and transgenic mice (29)] is sufficient to offer a level of protection against lipid-induced skeletal muscle insulin resistance. Given that 70–80% of insulin-stimulated glucose uptake is into muscle (17) and that a moderate increase in muscle expression of MnSOD is sufficient to have an effect on this, it follows that the improved glucose tolerance seen in HF diet-fed MnSOD transgenic mice studies could be driven largely by effects in muscle. The fact

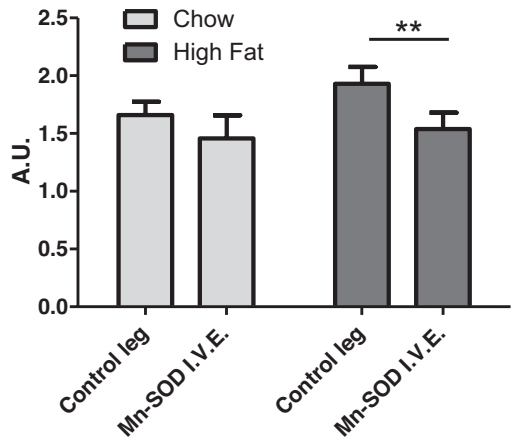

Fig. 4. Overexpression of MnSOD protects against increased protein carbonylation induced by a high-fat diet. Protein carbonylation levels in MnSOD overexpression and control muscles from chow- and high-fat diet-fed rats, as determined by enzymatic derivatization of the carbonyl groups into 2,4-dinitrophenylhydrazone by 2,4-dinitrophenylhydrazine, followed by resolution using PAGE and detection using a primary antibody to the dinitrophenylhydrazine moiety on the protein (n = 6/group). **$P < 0.01$.

that the HF diet-fed MnSOD transgenic mouse is not protected against hypertriglyceridemia, hyperlipidemia, or weight gain suggests that increased MnSOD in the liver and other tissues does not provide a wider physiological benefit (29). In our study, overexpression of MnSOD in muscle of chow-fed animals did not alter insulin-stimulated glucose uptake into muscle, whereas studies in cell culture suggested that elevation of MnSOD or mitochondrially targeted antioxidants could increase the insulin response in normal cells (29). This difference could be due to the lower degree of overexpression achieved here but may alternatively relate to differential effects on glutathione peroxidase and catalase activities since these were not evaluated in the tissue culture studies, and a moderate increase in cytosolic hydrogen peroxide seems to be insulin sensitizing (38, 48, 51). A further possibility is that cells were cultured at atmospheric oxygen concentrations (~159 mmHg), whereas the oxygen tension of in vivo muscle is closer to 15–25 mmHg (6, 45, 55). In the hyperoxygenated environment of cell culture, elevated oxidative protection via MnSOD may be of more importance to maintain metabolic function than in a normal physiological environment.

In this study, we did not observe a link between HF diet and MnSOD overexpression-induced alterations in insulin-stimulated muscle glucose uptake and changes in phosphorylation of insulin-signaling intermediates. Although it is possible that transient changes in phosphorylation of PI 3-kinase pathway intermediates may have been missed by making measurements in muscle harvested at the end of the clamp period (23), our studies are nevertheless consistent with others, suggesting that there can be a disconnect between the phosphorylation of PI 3-kinase pathway intermediates and translocation of the insulin-regulated glucose transporter GLUT4 or glucose uptake (7, 24, 28, 52). Specifically regarding MnSOD overexpression, our findings are consistent with those in L6 cells, where insulin resistance was ameliorated without significant modulation of insulin signaling (29). However, in another study of dexamethasone- or TNF-treated 3T3 adipocytes the mitochondrial antioxidant MnTBAP did enhance both insulin action and signaling, although insulin signaling was not investigated in accompanying in vivo studies, where treatment with Mn-TBAP improved glucose tolerance in *ob/ob* mice (30). In summary, it may be that altered subcellular compartmentalization or defective function of more distal components of the signaling pathway or trafficking events is of more significance in mediating the detected effects on insulin-stimulated glucose uptake.

The precise mechanism whereby ROS is able to antagonize insulin action in muscle is not clear at the present time. However, the restoration of glucose uptake in association with a reduction in protein carbonylation may offer some clue as to the mechanism whereby MnSOD is able to offer protection. Because protein carbonylation is a recognized marker of protein "damage," this could indicate a protective effect, opposing the activity of reactive species on modifying various proteins, including catalytic iron-containing enzymes (42), proteins of the mitochondrial electron transport chain (41), and signaling molecules (44). Identifying the specific detrimental posttranslational modifications, including carbonylation, on targeted metabolic proteins (Akt, AS160, and GLUT4) rather than on the proteome in general could offer a clearer mechanism for the protective effect of MnSOD overexpression. To this end, we examined the carbonylation state of IRS-1 and Akt but were unable to detect or show any change in carbonylation (data not shown).

It is also of interest to identify the key detrimental reactive species. Mitochondria contain enzymes known to be particular targets of superoxide (19) and other reactive oxygen and nitrogen species (26). In the present study, it may be that reactive species derived from superoxides other than hydrogen peroxide, such as peroxynitrite, may be reduced. Nitrogen oxidative species-induced posttranslational modifications have been identified in models of insulin resistance (10, 57), and thus it may be that these posttranslational modifications (reversible *S*-nitrosylation and permanent tyrosine nitration) are either more detrimental to protein function or more problematic to resolve (56).

In conclusion, the local overexpression of MnSOD in rat skeletal muscle in vivo was sufficient to partially protect the muscle against impaired glucose uptake and to decrease oxidative protein damage in animals exposed to a HF diet. This suggests that antioxidant molecules specifically targeting the mitochondria may be a future therapeutic option in the treatment of insulin resistance.

ACKNOWLEDGMENTS

We are grateful to D. Samocha-Bonet for critical comments on this manuscript, L. Wright, J. Reznick, T. Iseli, and M. Swarbrick for technical assistance, and the staff of the Biological Testing Facility.

GRANTS

This study was supported by the National Health and Medical Research Council (NHMRC) of Australia (Program Grant no. 535921). N. Turner is supported by a Career Development Award, G. J. Cooney and E. W. Kraegen by a Research Fellowship from the NHMRC of Australia, and M. E. Cleasby by a Wellcome Trust University Award.

DISCLOSURES

No conflicts of interest, financial or otherwise, are declared by the authors.

AUTHOR CONTRIBUTIONS

M.J.B., M.E.C., N.T., G.J.C., and E.W.K. did the conception and design of the research; M.J.B., A.E.B., J.D.T.-A., E.P., D.W., and E.S. performed the experiments; M.J.B., A.E.B., J.D.T.-A., E.P., D.W., E.S., and N.T. analyzed the data; M.J.B., A.E.B., J.D.T.-A., M.E.C., N.T., G.J.C., and E.W.K. interpreted the results of the experiments; M.J.B. prepared the figures; M.J.B. drafted the manuscript; A.E.B., M.E.C., N.T., G.J.C., and E.W.K. edited and revised the manuscript; A.E.B. and E.W.K. approved the final version of the manuscript.

REFERENCES

1. **Anderson EJ, Lustig ME, Boyle KE, Woodlief TL, Kane DA, Lin CT, Price JW 3rd, Kang L, Rabinovitch PS, Szeto HH, Houmard JA, Cortright RN, Wasserman DH, Neufer PD.** Mitochondrial H2O2 emission and cellular redox state link excess fat intake to insulin resistance in both rodents and humans. *J Clin Invest* 119: 573–581, 2009.
2. **Bachmann OP, Dahl DB, Brechtel K, Machann J, Haap M, Maier T, Loviscach M, Stumvoll M, Claussen CD, Schick F, Häring HU, Jacob S.** Effects of intravenous and dietary lipid challenge on intramyocellular lipid content and the relation with insulin sensitivity in humans. *Diabetes* 50: 2579–2584, 2001.
3. **Barrett WC, DeGnore JP, Keng YF, Zhang ZY, Yim MB, Chock PB.** Roles of superoxide radical anion in signal transduction mediated by reversible regulation of protein-tyrosine phosphatase 1b. *J Biol Chem* 274: 34543–34546, 1999.
4. **Beers RF Jr, Sizer IW.** A spectrophotometric method for measuring the breakdown of hydrogen peroxide by catalase. *J Biol Chem* 195: 133–140, 1952.

5. **Bloch-Damti A, Bashan N.** Proposed mechanisms for the induction of insulin resistance by oxidative stress. *Antioxid Redox Signal* 7: 1553–1567, 2005.
6. **Boegehold MA, Johnson PC.** Periarteriolar and tissue Po_2 during sympathetic escape in skeletal muscle. *Am J Physiol Heart Circ Physiol* 254: H929–H936, 1988.
7. **Boudina S, Sena S, Sloan C, Tebbi A, Han YH, O'Neill BT, Cooksey RC, Jones D, Holland WL, McClain DA, Abel ED.** Early mitochondrial adaptations in skeletal muscle to diet-induced obesity are strain dependent and determine oxidative stress and energy expenditure but not insulin sensitivity. *Endocrinology* 153: 2677–2688, 2012.
8. **Bruce CR, Hoy AJ, Turner N, Watt MJ, Allen TL, Carpenter K, Cooney GJ, Febbraio MA, Kraegen EW.** Overexpression of carnitine palmitoyltransferase-1 in skeletal muscle is sufficient to enhance fatty acid oxidation and improve high-fat diet-induced insulin resistance. *Diabetes* 58: 550–558, 2009.
9. **Bruce CR, Thrush AB, Mertz VA, Bezaire V, Chabowski A, Heigenhauser GJ, Dyck DJ.** Endurance training in obese humans improves glucose tolerance and mitochondrial fatty acid oxidation and alters muscle lipid content. *Am J Physiol Endocrinol Metab* 291: E99–E107, 2006.
10. **Carvalho-Filho MA, Ueno M, Hirabara SM, Seabra AB, Carvalheira JB, de Oliveira MG, Velloso LA, Curi R, Saad MJ.** S-nitrosation of the insulin receptor, insulin receptor substrate 1, and protein kinase b/akt: A novel mechanism of insulin resistance. *Diabetes* 54: 959–967, 2005.
11. **Chen X, Mele J, Giese H, Van Remmen H, Dollé ME, Steinhelper M, Richardson A, Vijg J.** A strategy for the ubiquitous overexpression of human catalase and CuZn superoxide dismutase genes in transgenic mice. *Mech Ageing Dev* 124: 219–227, 2003.
12. **Clark PW, Jenkins AB, Kraegen EW.** Pentobarbital reduces basal liver glucose output and its insulin suppression in rats. *Am J Physiol Endocrinol Metab* 258: E701–E707, 1990.
13. **Cleasby ME, Davey JR, Reinten TA, Graham MW, James DE, Kraegen EW, Cooney GJ.** Acute bidirectional manipulation of muscle glucose uptake by in vivo electrotransfer of constructs targeting glucose transporter genes. *Diabetes* 54: 2702–2711, 2005.
14. **Cleasby ME, Reinten TA, Cooney GJ, James DE, Kraegen EW.** Functional studies of akt isoform specificity in skeletal muscle in vivo; maintained insulin sensitivity despite reduced insulin receptor substrate-1 expression. *Mol Endocrinol* 21: 215–228, 2007.
15. **Czernichow S, Vergnaud AC, Galan P, Arnaud J, Favier A, Faure H, Huxley R, Hercberg S, Ahluwalia N.** Effects of long-term antioxidant supplementation and association of serum antioxidant concentrations with risk of metabolic syndrome in adults. *Am J Clin Nutr* 90: 329–335, 2009.
16. **Dalle-Donne I, Rossi R, Giustarini D, Gagliano N, Di Simplicio P, Colombo R, Milzani A.** Methionine oxidation as a major cause of the functional impairment of oxidized actin. *Free Radic Biol Med* 32: 927–937, 2002.
17. **DeFronzo RA, Jacot E, Jequier E, Maeder E, Wahren J, Felber JP.** The effect of insulin on the disposal of intravenous glucose. Results from indirect calorimetry and hepatic and femoral venous catheterization. *Diabetes* 30: 1000–1007, 1981.
18. **Doi T, Puri P, Bannigan J, Thompson J.** Pre-treatment with n-acetylcysteine upregulates superoxide dismutase 2 and catalase genes in cadmium-induced oxidative stress in the chick omphalocele model. *Pediatr Surg Int* 27: 131–136, 2011.
19. **Flint DH, Tuminello JF, Emptage MH.** The inactivation of Fe-S cluster containing hydro-lyases by superoxide. *J Biol Chem* 268: 22369–22376, 1993.
20. **Flohe L, Gunzler WA.** Assays of glutathione peroxidase. *Methods Enzymol* 105: 114–121, 1984.
21. **Flohe L, Otting F.** Superoxide dismutase assays. *Methods Enzymol* 105: 93–104, 1984.
22. **Franco AA, Odom RS, Rando TA.** Regulation of antioxidant enzyme gene expression in response to oxidative stress and during differentiation of mouse skeletal muscle. *Free Radic Biol Med* 27: 1122–1132, 1999.
23. **Frangioudakis G, Ye JM, Cooney GJ.** Both saturated and n-6 polyunsaturated fat diets reduce phosphorylation of insulin receptor substrate-1 and protein kinase b in muscle during the initial stages of in vivo insulin stimulation. *Endocrinology* 146: 5596–5603, 2005.
24. **Fröjdö S, Vidal H, Pirola L.** Alterations of insulin signaling in type 2 diabetes: a review of the current evidence from humans. *Biochim Biophys Acta* 1792: 83–92, 2009.
25. **García-Macia M, Vega-Naredo I, De Gonzalo-Calvo D, Rodríguez-González SM, Camello PJ, Camello-Almaraz C, Martín-Cano FE, Rodríguez-Colunga MJ, Pozo MJ, Coto-Montes AM.** Melatonin induces neural SOD2 expression independent of the NF-kappaB pathway and improves the mitochondrial population and function in old mice. *J Pineal Res* 50: 54–63, 2011.
26. **Gardner PR.** Superoxide-driven aconitase Fe-S center cycling. *Biosci Rep* 17: 33–42, 1997.
27. **Gurney ME, Pu H, Chiu AY, Dal Canto MC, Polchow CY, Alexander DD, Caliendo J, Hentati A, Kwon YW, Deng HX, Chen W, Zhai P, Sufit RL, Siddique T.** Motor neuron degeneration in mice that express a human Cu,Zn superoxide dismutase mutation. *Science* 264: 1772–1775, 1994.
28. **Hoehn KL, Hohnen-Behrens C, Cederberg A, Wu LE, Turner N, Yuasa T, Ebina Y, James DE.** IRS1-independent defects define major nodes of insulin resistance. *Cell Metab* 7: 421–433, 2008.
29. **Hoehn KL, Salmon AB, Hohnen-Behrens C, Turner N, Hoy AJ, Maghzal GJ, Stocker R, Van Remmen H, Kraegen EW, Cooney GJ, Richardson AR, James DE.** Insulin resistance is a cellular antioxidant defense mechanism. *Proc Natl Acad Sci USA* 106: 17787–17792, 2009.
30. **Houstis N, Rosen ED, Lander ES.** Reactive oxygen species have a causal role in multiple forms of insulin resistance. *Nature* 440: 944–948, 2006.
31. **Hoy AJ, Bruce CR, Cederberg A, Turner N, James DE, Cooney GJ, Kraegen EW.** Glucose infusion causes insulin resistance in skeletal muscle of rats without changes in Akt and AS160 phosphorylation. *Am J Physiol Endocrinol Metab* 293: E1358–E1364, 2007.
32. **James DE, Jenkins AB, Kraegen EW.** Heterogeneity of insulin action in individual muscles in vivo: euglycemic clamp studies in rats. *Am J Physiol Endocrinol Metab* 248: E567–E574, 1985.
33. **Kennaway DJ, Varcoe TJ, Mau VJ.** Rhythmic expression of clock and clock-controlled genes in the rat oviduct. *Mol Hum Reprod* 9: 503–507, 2003.
34. **Kim JA, Wei Y, Sowers JR.** Role of mitochondrial dysfunction in insulin resistance. *Circ Res* 102: 401–414, 2008.
35. **Kraegen EW, Clark PW, Jenkins AB, Daley EA, Chisholm DJ, Storlien LH.** Development of muscle insulin resistance after liver insulin resistance in high-fat-fed rats. *Diabetes* 40: 1397–1403, 1991.
36. **Kraegen EW, James DE, Jenkins AB, Chisholm DJ.** Dose-response curves for in vivo insulin sensitivity in individual tissues in rats. *Am J Physiol Endocrinol Metab* 248: E353–E362, 1985.
37. **Livak KJ, Schmittgen TD.** Analysis of relative gene expression data using real-time quantitative PCR and the 2[−Delta Delta C(T)] Method. *Methods* 25: 402–408, 2001.
38. **Loh K, Deng H, Fukushima A, Cai X, Boivin B, Galic S, Bruce C, Shields BJ, Skiba B, Ooms LM, Stepto N, Wu B, Mitchell CA, Tonks NK, Watt MJ, Febbraio MA, Crack PJ, Andrikopoulos S, Tiganis T.** Reactive oxygen species enhance insulin sensitivity. *Cell Metab* 10: 260–272, 2009.
39. **MacArthur DG, Seto JT, Chan S, Quinlan KG, Raftery JM, Turner N, Nicholson MD, Kee AJ, Hardeman EC, Gunning PW, Cooney GJ, Head SI, Yang N, North KN.** An actn3 knockout mouse provides mechanistic insights into the association between alpha-actinin-3 deficiency and human athletic performance. *Hum Mol Genet* 17: 1076–1086, 2008.
40. **McClung JP, Roneker CA, Mu W, Lisk DJ, Langlais P, Liu F, Lei XG.** Development of insulin resistance and obesity in mice overexpressing cellular glutathione peroxidase. *Proc Natl Acad Sci USA* 101: 8852–8857, 2004.
41. **Meany DL, Xie H, Thompson LV, Arriaga EA, Griffin TJ.** Identification of carbonylated proteins from enriched rat skeletal muscle mitochondria using affinity chromatography-stable isotope labeling and tandem mass spectrometry. *Proteomics* 7: 1150–1163, 2007.
42. **Namgaladze D, Hofer HW, Ullrich V.** Redox control of calcineurin by targeting the binuclear Fe(2+)-Zn(2+) center at the enzyme active site. *J Biol Chem* 277: 5962–5969, 2002.
43. **Namgaladze D, Shcherbyna I, Kienhöfer J, Hofer HW, Ullrich V.** Superoxide targets calcineurin signaling in vascular endothelium. *Biochem Biophys Res Commun* 334: 1061–1067, 2005.
44. **Nomiyama T, Igarashi Y, Taka H, Mineki R, Uchida T, Ogihara T, Choi JB, Uchino H, Tanaka Y, Maegawa H, Kashiwagi A, Murayama K, Kawamori R, Watada H.** Reduction of insulin-stimulated glucose uptake by peroxynitrite is concurrent with tyrosine nitration of insulin receptor substrate-1. *Biochem Biophys Res Commun* 320: 639–647, 2004.
45. **Prewitt RL, Johnson PC.** The effect of oxygen on arteriolar red cell velocity and capillary density in the rat cremaster muscle. *Microvasc Res* 12: 59–70, 1976.

46. **Qiu X, Brown K, Hirschey MD, Verdin E, Chen D.** Calorie restriction reduces oxidative stress by sirt3-mediated sod2 activation. *Cell Metab* 12: 662–667, 2011.
47. **Reaven GM.** Banting lecture 1988. Role of insulin resistance in human disease. *Diabetes* 37: 1595–1607, 1988.
48. **Rhee SG.** Cell signaling. H2O2, a necessary evil for cell signaling. *Science* 312: 1882–1883, 2006.
49. **Tam CS, Viardot A, Clément K, Tordjman J, Tonks K, Greenfield JR, Campbell LV, Samocha-Bonet D, Heilbronn LK.** Short-term overfeeding may induce peripheral insulin resistance without altering subcutaneous adipose tissue macrophages in humans. *Diabetes* 59: 2164–2170, 2010.
50. **Taylor ER, Hurrell F, Shannon RJ, Lin TK, Hirst J, Murphy MP.** Reversible glutathionylation of complex I increases mitochondrial superoxide formation. *J Biol Chem* 278: 19603–19610, 2003.
51. **Tonks NK.** Protein tyrosine phosphatases: from genes, to function, to disease. *Nat Rev Mol Cell Biol* 7: 833–846, 2006.
52. **Tremblay F, Lavigne C, Jacques H, Marette A.** Defective insulin-induced GLUT4 translocation in skeletal muscle of high fat-fed rats is associated with alterations in both Akt/protein kinase B and atypical protein kinase C (zeta/lambda) activities. *Diabetes* 50: 1901–1910, 2001.
53. **Turner N, Bruce CR, Beale SM, Hoehn KL, So T, Rolph MS, Cooney GJ.** Excess lipid availability increases mitochondrial fatty acid oxidative capacity in muscle: evidence against a role for reduced fatty acid oxidation in lipid-induced insulin resistance in rodents. *Diabetes* 56: 2085–2092, 2007.
54. **Veal EA, Day AM, Morgan BA.** Hydrogen peroxide sensing and signaling. *Mol Cell* 26: 1–14, 2007.
55. **Whalen WJ, Buerk D, Thuning CA.** Blood flow-limited oxygen consumption in resting cat skeletal muscle. *Am J Physiol* 224: 763–768, 1973.
56. **White PJ, Charbonneau A, Cooney GJ, Marette A.** Nitrosative modifications of protein and lipid signaling molecules by reactive nitrogen species. *Am J Physiol Endocrinol Metab* 299: E868–E878, 2010.
57. **Yasukawa T, Tokunaga E, Ota H, Sugita H, Martyn JA, Kaneki M.** S-nitrosylation-dependent inactivation of Akt/protein kinase B in insulin resistance. *J Biol Chem* 280: 7511–7518, 2005.
58. **Yen HC, Oberley TD, Vichitbandha S, Ho YS, St Clair DK.** The protective role of manganese superoxide dismutase against adriamycin-induced acute cardiac toxicity in transgenic mice. *J Clin Invest* 98: 1253–1260, 1996.

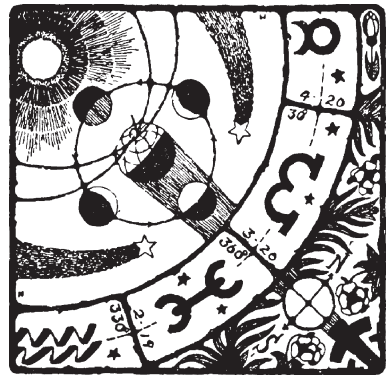

Overexpression of manganese superoxide dismutase ameliorates high-fat diet-induced insulin resistance in rat skeletal muscle

Michael J. Boden, Amanda E. Brandon, Jennifer D. Tid-Ang, Elaine Preston, Donna Wilks, Ella Stuart, Mark E. Cleasby, Nigel Turner, Gregory J. Cooney and Edward W. Kraegen

Am J Physiol Endocrinol Metab 303:E798-E805, 2012. First published 24 July 2012;
doi: 10.1152/ajpendo.00577.2011